Cerebral Cortex February 2013;23:378–388
doi:10.1093/cercor/bhs027
Advance Access publication February 17, 2012

An Ion Transport-Independent Role for the Cation-Chloride Cotransporter KCC2 in Dendritic Spinogenesis In Vivo

Hubert Fiumelli[1], Adrian Briner[2,3,4], Martin Puskarjov[5,6], Peter Blaesse[5,6], Bebyanda JT Belem[2,3,4], Alex G Dayer[3,4,7], Kai Kaila[5,6], Jean-Luc Martin[1] and Laszlo Vutskits[2,3,4]

[1]Center for Psychiatric Neurosciences, Department of Psychiatry, Lausanne University Hospital, 1008 Prilly-Lausanne, Switzerland, [2]Department of Anesthesiology, Pharmacology and Intensive Care, University Hospital of Geneva, 1211 Geneva 4, Switzerland, [3]Department of Fundamental Neurosciences and [4]Geneva Neuroscience Center, University of Geneva Medical School, 1204 Geneva, Switzerland, [5]Department of Biosciences and [6]Neuroscience Center, University of Helsinki, 00014 Helsinki, Finland and [7]Department of Mental Health and General Psychiatry, University Hospital of Geneva, 1211 Geneva 4, Switzerland

Hubert Fiumelli and Adrian Briner have contributed equally to this work

Address correspondence to Laszlo Vutskits, Department of Anesthesiology, Pharmacology and Intensive Care, University Hospital of Geneva, 4, rue Gabrielle-Perret-Gentil, 1211 Geneva 4, Switzerland. Email: laszlo.vutskits@unige.ch and to Jean-Luc Martin, Center for Psychiatric Neurosciences, Department of Psychiatry, Lausanne University Hospital, 1008 Prilly-Lausanne, Switzerland. Email: jean-luc.martin@unil.ch.

The neuron-specific K-Cl cotransporter, KCC2, is highly expressed in the vicinity of excitatory synapses in pyramidal neurons, and recent in vitro data suggest that this protein plays a role in the development of dendritic spines. The in vivo relevance of these observations is, however, unknown. Using in utero electroporation combined with post hoc iontophoretic injection of Lucifer Yellow, we show that premature expression of KCC2 induces a highly significant and permanent increase in dendritic spine density of layer 2/3 pyramidal neurons in the somatosensory cortex. Whole-cell recordings revealed that this increased spine density is correlated with an enhanced spontaneous excitatory activity in KCC2-transfected neurons. Precocious expression of the N-terminal deleted form of KCC2, which lacks the chloride transporter function, also increased spine density. In contrast, no effect on spine density was observed following in utero electroporation of a point mutant of KCC2 (KCC2-C568A) where both the cotransporter function and the interaction with the cytoskeleton are disrupted. Transfection of the C-terminal domain of KCC2, a region involved in the interaction with the dendritic cytoskeleton, also increased spine density. Collectively, these results demonstrate a role for KCC2 in excitatory synaptogenesis in vivo through a mechanism that is independent of its ion transport function.

Keywords: cortex, development, GABA, plasticity, synaptogenesis

Introduction

Neuronal dendritic arbor development and synaptogenesis are crucial steps in the assembly and maintenance of functional brain circuitry. In the cerebral cortex of rhesus monkey, where the timing, magnitude, and rate of synapse production have been extensively described, the most intense phase of synaptogenesis takes place during the perinatal period when an up to 17-fold increase in synapse number occurs within a few months (reviewed in Rakic et al. 1994). In humans, comparable expansion in the number of synapses is observed between the third trimester of pregnancy and the first few years of postnatal life (Huttenlocher and Dabholkar 1997; Petanjek et al. 2011). In contrast, the peak synaptogenic period is limited to a narrower time window in rodents and happens between the second and fourth postnatal weeks (Juraska 1982; De Felipe et al. 1997). In these species, the perinatal exponential synaptic growth leads to an initial overproduction of synapses and then to a selective pruning of synaptic contacts extending from puberty to adolescence and beyond (Juraska 1982; Rakic et al. 1994; Petanjek et al. 2011).

Dendritic spines are small protrusions from dendrites that bear the postsynaptic sites of most excitatory contacts on pyramidal neurons and are particularly well suited to study the multifaceted aspects of excitatory synaptogenesis. Increases in dendritic spine density closely parallel excitatory synaptogenesis during development (Juraska 1982; De Felipe et al. 1997). Electron microscopic observations have shown that the vast majority of dendritic spines receive presynaptic contacts, and there is now evidence that newly generated spines can rapidly form functional synapses and integrate into functional circuitries (De Roo et al. 2009; Kwon and Sabatini 2011). Importantly, links between spine morphology and synaptic function have been reported (Arellano et al. 2007). Among them, spine head volume has been shown to be directly proportional to the size of postsynaptic density, the number of postsynaptic receptors, the number of docked vesicles in the presynaptic terminal, and thus the readily releasable pool of neurotransmitters (Harris and Stevens 1989; Nusser et al. 1998; Schikorski and Stevens 1999; Schikorski and Stevens 2001). Of clinical relevance, altered dendritic spine density and morphology have been reported in several neurological and psychiatric disorders (Penzes et al. 2011).

The intimate temporal coincidence between the developmental onset of KCC2 expression and the most intense phase of synaptogenesis during the brain growth spurt (Juraska 1982; De Felipe et al. 1997) points to a possible role for this cotransporter in synapse formation. In support of this hypothesis, an increasing number of observations suggest that KCC2 may play a role in the formation of dendritic spines. Indeed, immunocytochemical visualization of KCC2 at the subcellular level of pyramidal neurons revealed that this cotransporter is highly expressed in and close to dendritic spines (Gulyas et al. 2001; Bartho et al. 2004; Baldi et al. 2010). Accordingly, recent in vitro data propose a role for KCC2 in excitatory synaptogenesis (Li et al. 2007). In these experiments performed in primary cortical cultures, KCC2 promoted dendritic spine development independent of its chloride transporter function, through an interaction with the actin cytoskeleton. This mechanism is in-line with recent observations suggesting a role for KCC2 during central nervous system development that is independent of its ion cotransport function (Horn et al. 2010).

In vivo evidence for a role of KCC2 in excitatory synaptogenesis is, however, lacking. In this study, we addressed this issue by focusing on dendritic spine development of layer 2/3 pyramidal neurons in the rat somatosensory cortex (SSC). Using a combination of in utero electroporation and iontophoretic injection of Lucifer Yellow (LY), we demonstrate that premature expression of KCC2 induces a highly significant and permanent increase in dendritic spine density of these principal cells. Whole-cell recordings revealed that the KCC2-induced increase in spine density correlates with enhanced spontaneous excitatory synaptic activity. Increased spinogenesis was also observed following expression of the N-terminal deleted form of KCC2, which lacks the chloride transporter function, as well as upon expression of the C-terminal domain of KCC2, implicated in the interaction between KCC2 and the actin cytoskeleton. In contrast, no effect on spine density was observed following electroporation of a point mutant of KCC2 (KCC2-C568A) where both the cotransporter function and the interaction with the cytoskeleton are disrupted. Altogether, these results indicate a structural role of KCC2 in excitatory synaptogenesis in cortical neurons in vivo.

Materials and Methods

The experimental protocol was conducted according to the guidelines of the Swiss Federal Veterinary Office and was approved by the cantonal Animal Welfare Committee. The electrophysiological experiments were done using methods approved by the University of Helsinki Animal Care and Use Committee. Wistar rats (Charles River, Arbresle, France) were housed and bred in the animal facilities under a 12 h light/dark cycle and temperature-controlled (22 ± 2 °C) conditions. Food and water were available ad libitum.

In Utero Electroporation

In utero electroporation was performed according to Saito and Nakatsuji (2001) with minor modifications. Briefly, timed pregnant Wistar rats with E17.5 embryos were anaesthetized with isoflurane (3.5% induction, 2% during the surgery), and uterine horns were successively exposed after a midline laparotomy. All embryos were injected with 1–1.5 μL plasmid DNA solution (prepared in 0.9% NaCl, 0.3 mg/mL Fast Green [Sigma]) into a lateral ventricle through the uterine membrane. The plasmid pCAG-IRES-EGFP (0.8 μg/μL) was injected alone or, for coelectroporation, together with a vector encoding wild-type (WT) or mutant forms of KCC2 (2.2 μg/μL). Cells were electroporated by holding the head of each embryo between tweezers-style circular electrodes (7 mm diameter, Harvard Apparatus) across the uterus wall while 5 pulses (50 V, 50-ms duration at 100-ms intervals) were delivered with a square-wave generator (ECM 830; Harvard Apparatus). The uterine horns were returned into the abdominal cavity, the wall and skin were sutured, and the embryos were allowed to resume normal development.

Expression Vectors for In Utero Electroporation

The WT KCC2, KCC2-C568A, and KCC2-ΔNTD expressing constructs were generated by subcloning the respective KCC2 variant sequences into pCAG, a vector bearing a modified chicken β-actin promoter with a cytomegalovirus immediate-early enhancer that directs elevated and persistent expression levels in both precursors and postmitotic neurons (Niwa et al. 1991). The pCAG acceptor plasmid was engineered by removing the IRES-EGFP sequence from the pCAG-IRES-EGFP vector (Cancedda et al. 2007). The rat full-length WT and KCC2-C568A cDNAs have been previously described (Fiumelli et al. 2005; Cancedda et al. 2007) and the pCAG-KCC2-ΔNTD as well as the pCAG-KCC2-CTD constructs were described in Li et al. (2007). In this study, the pCAG-IRES-EGFP plasmid (Cancedda et al. 2007) was coinjected to fluorescently tag electroporated cells.

Iontophoretic Post Hoc Single Cell Injections

Animals were sacrificed at defined time points by an intraperitoneal overdose of pentobarbital (100 mg/kg) and perfused transcardially with a 4% paraformaldehyde and 0.125% glutaraldehyde solution (pH 7.4). Brains were then removed and postfixed for 2 h in 4% paraformaldehyde. Coronal sections of 300 μm thickness were then cut on a vibratome in ice-cold phosphate-based saline solution (PBS, pH 7.4). Coronal sections were prestained for 30 min with methylene blue, which enables the visualization of neuronal somata, mounted into an injection chamber, and placed on the fixed stage of a Zeiss microscope equipped with a micromanipulator. Layer 2/3 pyramidal neurons were loaded iontophoretically with a 5% LY solution (Sigma–Aldrich, St. Louis, MO) using sharp micropipettes with a negative current of 70 nA. Loading time per cell was 4 min, 6–9 cells were injected per slice, and we used 2 slices per animal and 3 animals per experimental group.

Immunohistochemistry

For immunolabeling, coronal sections were incubated with the appropriate primary antibody for 48 h at ambient temperature in a PBS solution containing sucrose (5%), bovine serum albumin (2%), Triton-X100 (1%), and sodium azide (0.1%). Slices were then rinsed in PBS solution and incubated for an additional 48 h with Alexa-conjugated secondary antibodies (Molecular Probes, Carlsbad, CA 1:1000). Slices were mounted and coverslipped using immunomount (Thermo scientific, Pittsburgh, PA). The following primary antibodies were used: anti-LY antibody (Sigma–Aldrich; 1:5000 dilution), rabbit anti-GFP antibody (ion-exchange purified IgG fraction, Invitrogen, Carlsbad, CA; 1:1000 dilution), mouse anti-GFP antibody (Chemicon, 1:500 dilution), and rabbit anti-KCC2 antibody (Milipore, 1:200).

Analysis of Neuronal Cytoarchitecture

Only pyramidal neurons lying within layer 2/3 of the SSC with proper filling of distal dendritic tips were included into the analysis. Reconstruction of the 3D dendritic arbor structure was performed using a computer-based Neurolucida system (Microbrightfield, Williston, VT) with a ×40 objective on a Nikon microscope (Nikon Corporation, Tokyo, Japan). In each experimental group, total dendritic length, number of branching points, and Sholl's distribution for both basal and apical dendritic arbors were quantified by an observer blind to the experimental conditions. An LSM 510 meta confocal microscope (Carl–Zeiss, Göttingen, Germany) equipped with a ×63 oil-immersion objective was used for dendritic spine analysis. Spine analysis was performed on acquired stacks of images using a homemade plug-in written for OsiriX software (Pixmeo, Geneva, Switzerland). This plug-in allows precise spine quantification, individual tagging, and measurement in 3D by scrolling through the *z*-axis. We defined spines as structures emerging from the dendrites that were longer than 0.4 μm and for which we could distinguish an enlargement at the tip (spine head). Spines head diameters were measured at their largest width in *xy*-axis on the z-image corresponding to the central axis of the spine head.

Note that for illustration purposes, images presented in figures are maximum intensity projections of z stacks with volume rendering, further treated with a Gaussian blur filter.

Electrophysiology

Acute 400-μm coronal neocortical slices were prepared from postnatal day (PND) 30–34 in utero electroporated Wistar rats. Prior to decapitation, anesthesia was induced using halothane (Sigma, Germany). Brains were quickly removed and immersed into an ice-cold sucrose-based sectioning solution containing (in mM): 87 NaCl, 2.5 KCl, 0.5 $CaCl_2$, 25 $NaHCO_3$, 1.25 NaH_2PO_4, 7 $MgCl_2$, 50 sucrose, and 25 D-glucose, equilibrated with 95% O_2 and 5% CO_2. Slices were cut with a VT 1000s vibrating blade microtome (Leica, Germany). Before the experiments were started, the slices were allowed to recover at 36 °C for 1 h in recovery solution containing (in mM): 124 NaCl, 3 KCl, 2 $CaCl_2$, 25 $NaHCO_3$, 1.1 NaH_2PO_4, 2 $MgSO_4$, 6 $MgCl_2$, and 10 D-glucose, equilibrated with 95% O_2 and 5% CO_2.

Miniature excitatory postsynaptic currents (mEPSCs) were recorded in whole-cell voltage-clamp configuration at 32 °C from 12 pairs (10 slices, 6 animals) of cortical layer 2/3 pyramidal neurons. Each pair consisted of an EGFP-positive neuron coelectroporated with pCAG-KCC2 and pCAG-IRES-EGFP constructs and a neighboring EGFP-negative control neuron located up to 50 μm away. EGFP fluorescence was excited at 488 nm and recorded with a 530 nm band-pass filter using a Radiance 2100 confocal microscope (Bio-Rad, UK). The composition of the extracellular solution was (in mM): 124 NaCl, 3 KCl, 2 $CaCl_2$, 25 $NaHCO_3$, 1.1 NaH_2PO_4, 2 $MgSO_4$, and 10 D-glucose, 0.02 bicuculline methiodide, and 0.002 tetrodotoxin citrate, equilibrated with 95% O_2 and 5% CO_2, pH 7.4. Patch-clamp recordings were obtained using an EPC 10 amplifier (HEKA Elektronik, Germany). Patch pipettes were fabricated from borosilicate glass (Harvard Apparatus, UK), and their resistance ranged from 4 to 5.5 MΩ. The pipette solution consisted of (in mM): 18 KCl, 111 K-gluconate, 0.5 $CaCl_2$, 2 NaOH, 10 glucose, 10 HEPES, 2 Mg-ATP, 5 BAPTA, and pH was adjusted to 7.3 with KOH. Membrane potential was held at −70 mV. Each neuron was allowed to equilibrate with the pipette solution for 5 min before mEPSC recordings took place. Only cells with stable access resistance throughout the recording were accepted for analysis. Epochs of 300–600 s were recorded. The average frequency and amplitude of mEPSCs was analyzed using WinEDR software (Dr John Dempster, University of Strathclyde, UK).

Statistics

All statistics are presented as the mean ± the standard error of mean. Normality was tested for each distribution (D'Agostino and Pearson test), and α was set to 5% for all tests. For multiple comparisons, statistical significance was determined using one-way analysis of variance followed by Bonferroni post hoc tests (Prism Software version 5.0a, GraphPad Inc, La Jolla, CA). Where appropriate, two-tailed Student's *t*-test was performed. Statistical significance in the mEPSC experiments was analyzed using the nonparametric Wilcoxon matched pairs test (StatPlus 2009, AnalystSoft). $P < 0.05$ was considered as statistically significant.

Results

Dendritic Arbor Development and Spinogenesis of Layer 2/3 Pyramidal Neurons in the Early Postnatal Period

To elucidate the role of KCC2 during neuronal differentiation and synaptogenesis, we focused on dendritic arbor and spine development of layer 2/3 pyramidal neurons in the SSC. Since detailed quantitative description regarding the early postnatal development of these cells is as yet unavailable, we first investigated this issue using iontophoretic single cell injections of LY at distinct developmental time points extending from PND 5 to 90. This approach, allowing complete filling of apical and basal dendrites with dendritic spines (Briner et al. 2010), revealed an approximately 4-fold increase in apical (409 ± 31%) and a 6.5-fold increase in basal (670 ± 24%) dendritic arbor lengths during this period (Fig. 1*A–B*). The most intense phase of arbor differentiation was observed between PND 5 and 10, when fast dendritic growth (260 ± 17%, $P = 0.0001$ and 380 ± 11, $P < 0.0001$; apical and basal dendritic lengths, respectively) was accompanied with a highly significant increase in the number of branching points on either apical (6.4 ± 0.4 vs. 13 ± 0.8, $P = 0.0004$) or basal (3.6 ± 0.4 vs. 14.6 ± 0.9, $P < 0.0001$) trees (Fig. 1*B–C*). In the apical arbor, no further increase in branch point number was found following PND 10, and dendritic length analysis revealed no significant arbor expansion following PND 15 (Fig. 1*B–C*). In contrast, the basal dendritic tree displayed significant increases in branching between PND 10 and 15 ($P = 0.022$), as well as further significant enhancement of dendritic length up to PND 90 ($P = 0.002$) (Fig. 1*B–C*).

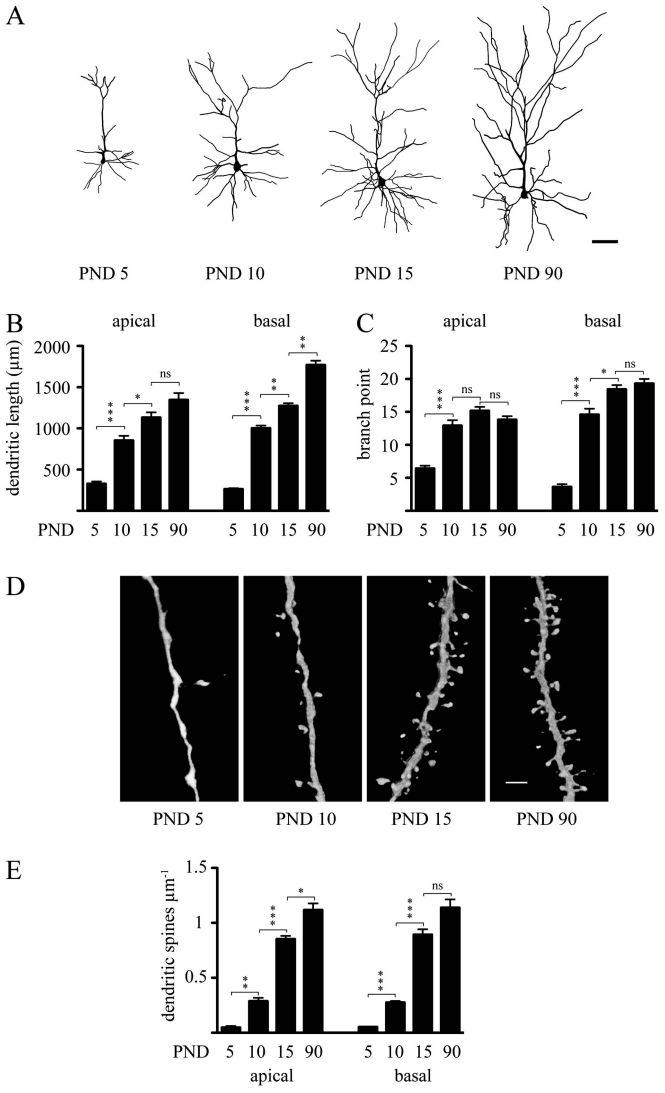

Figure 1. Dendritic arbor and spine development of layer 2/3 pyramidal neurons in the SSC. (*A*) Representative Neurolucida reconstructions of LY-injected pyramidal neurons in layer 2/3 of the SSC at PNDs 5, 10, 15, and 90 showing the temporal evolution of dendritic arborization pattern and spinogenesis during the first three postnatal months. (*B*) Quantitative analysis describing the temporal evolution of apical and basal dendritic lengths, and (*C*) branching points. (*D*) Representative confocal images (3D volume rendering) showing the temporal evolution of dendritic spine density on apical dendritic shafts of layer 2/3 pyramidal neurons. (*E*) Quantitative analysis of the temporal evolution of dendritic spine density on second order apical and basal dendritic shafts. Results are expressed as mean ± standard error of mean, $n = 3$ animals per age group. A total of 8–12 injected cells per age group were randomly selected for arbor analysis. A total of 2580 spines for apical and 2631 spines for basal dendrites were counted to determine spine density. One-way ANOVA with Bonferroni post hoc test was used to assess statistical differences between age groups either in apical or in basal dendrites. $^*P < 0.05$; $^{**}P < 0.01$; $^{***}P < 0.001$ compared with the dendritic arborization (*B–C*) or spine density (*E*) of the previous age group. PND: postnatal day scale bar: 100 μm in A; 6 μm in D; ns, nonsignificant difference.

Since dendritic spines represent primary sites of excitatory synaptic contacts on pyramidal neurons and intense synaptogenesis in the rodent SSC has been reported during the first month of postnatal life (Juraska 1982), we next focused on temporal evolution of dendritic spine density on layer 2/3 pyramidal neurons in the SSC. Confocal microscopic analysis of

dendritic spine development on second-order dendritic shafts of these LY-loaded cells revealed a more than 20-fold increase in dendritic spine density between PND 5 and 90, with comparable effects on apical (2236 ± 147%, $P < 0.0001$) and basal (2280 ± 184%, $P = 0.0001$) dendritic segments (Fig. 1*D–E*). At PND 5, only a very small number of dendritic protrusions were detectable which significantly increased by PND 10 on either apical (from 0.05 ± 0.01 to 0.29 ± 0.03 μm^{-1}; $P = 0.0019$) and basal (from 0.05 ± 0.003 to 0.28 ± 0.01 μm^{-1}; $P < 0.0001$) dendritic shafts. A further, highly significant increase in dendritic spine density was found at PND 15 (apical: 0.85 ± 0.03 μm^{-1}, $P = 0.0002$; basal: 0.89 ± 0.05 μm^{-1}, $P = 0.0003$). The number of spines still increased, although to a lower extent, by PND 90 (apical: 1.12 ± 0.06 μm^{-1}, $P = 0.02$; basal: 1.14 ± 0.07 μm^{-1}, $P = 0.051$).

The Electroporation Procedure Per Se Does Not Interfere with Physiological Patterns of Dendritic Arbor and Spine Development

In utero electroporation is a powerful tool to examine the role of genes in the establishment of an appropriately wired cerebral cortex (LoTurco et al. 2009). However, neuronal development is exquisitely sensitive to physiological and nonphysiological external stimuli (Hensch 2004). In this regard, since in utero electroporation includes potential harmful conditions, such as electric pulses, anesthesia, and perisurgical stress, we tested whether this procedure affected physiological patterns of dendritic arbor and spine development. To rule out this issue, we injected an EGFP-expressing plasmid into one of the lateral ventricles of E17.5 rat embryos and transferred this vector into neural progenitor cells by in utero electroporation as previously described (Saito and Nakatsuji 2001; Cancedda et al. 2007). Consistent with previous reports (Cancedda et al. 2007), EGFP-expressing layer 2/3 pyramidal neurons were observed in the postnatal SSC (Figs. 2*A,B* and 3*A,B*). Accurate dendritic arbor tracing as well as dendritic spine analysis of EGFP-labeled neurons were, however, hindered by the close proximity of a relatively large number of pyramidal neurons with highly overlapping dendritic arbor (Fig. 2*A*). To circumvent this technical problem and to evaluate the impact of in utero electroporation per se on dendritic arbor and spine development, we performed iontophoretic injections of LY into a randomly selected number of EGFP-labeled neurons as well as into EGFP-negative layer 2/3 pyramidal neurons (i.e., sham controls) in the proximity of EGFP-positive, LY-injected cells in cortical slices obtained at PND 15 from electroporated animals (Fig. 2*B*). This approach allowed us to compare dendritic arbor and spine architecture between layer 2/3 pyramidal neurons electroporated in the presence or the absence of EGFP-expressing plasmid within the same cortical microenvironment (Fig. 2*C–E*). As shown in Figure 2*F,G*, no significant difference in dendritic arbor morphology was observed between EGFP-positive and EGFP-negative pyramidal neurons. Importantly, the dendritic tree of these EGFP-expressing neurons was comparable to that of layer 2/3 pyramidal neurons from animals that were not subjected to in utero electroporation. Confocal analysis revealed no significant differences in terms of dendritic spine density between these 3 groups (Fig. 2*H,I*), providing evidence that the in utero electroporation procedure per se does not impair physiological patterns of dendritic arbor and spine development of layer 2/3 pyramidal neurons. Thus, for the remainder of this study, EGFP-negative neurons located in the vicinity of EGFP-labeled neurons expressing KCC2 or a mutant form of KCC2 will be used as controls.

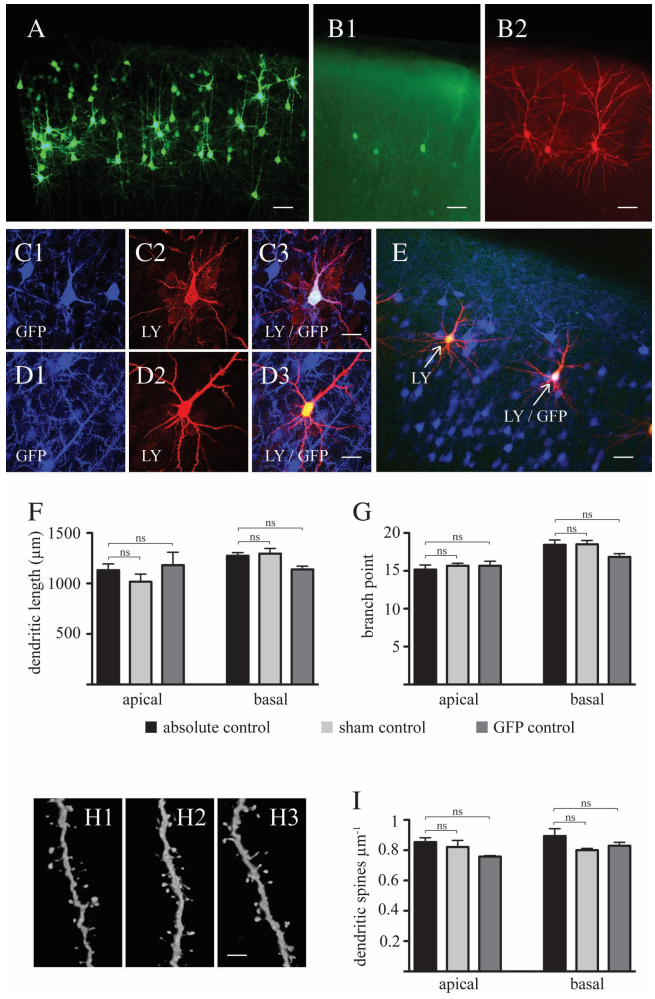

Figure 2. In utero electroporation of enhanced green fluorescent protein at gestational day 17.5 labels of layer 2/3 pyramidal neurons without affecting physiological patterns of dendritic arbor and spine development. (*A*) Low-magnification micrographs, following immunohistochemistry with an antibody against EGFP, showing the presence of labeled layer 2/3 pyramidal neurons in the SSC at PND 15. (*B*) Detailed dendritic arbor architecture of EGFP-expressing cells (*B1*, without antibody-induced enhancement of fluorescence intensity) can be revealed by iontophoretic injections of LY into these cells (*B2*). (*C*) Injection of LY into EGFP-positive (*C1*: EGFP, *C2*: LY, and *C3*: colocalization) and into (*D*) EGFP-negative cells (*D1*: EGFP, *D2*: LY, and *D3*: colocalization) allows detection and analysis of adjacent control and electroporated cells in the same microenvironment (*E*). Quantitative analysis of dendritic length (*F*) and branch points (*G*) at PND 15 reveals no difference in gross dendritic arbor architecture between absolute controls (i.e., neurons from nonelectroporated animals), sham controls (i.e., nonelectroporated cells from animals which underwent the electroporation procedure), and electroporated cells. (*H*) Representative micrographs of dendritic spines (*H1*: absolute control, *H2*: sham control, *H3*: EGFP-expressing group), and (*I*) quantitative analysis of spine density demonstrate no difference between these three groups. Results are expressed as mean ± standard error of mean, $n = 3$ animals per experimental group. A total of 8–12 injected cells per experimental group were randomly selected for arbor analysis. A total of 3183 spines for apical and 3298 spines for basal dendrites were counted to determine spine density. One-way ANOVA with Bonferroni post hoc test was used to assess statistical differences between age groups either in apical or in basal dendrites. EGFP, enhanced green fluorescent protein; ns, nonsignificant difference; Scale bars: *A–B*, *E*: 100 μm; *C–D*: 40 μm; *H*: 6 μm.

In Utero Electroporation of KCC2 Permanently Increases Dendritic Spine Density

To study the role of KCC2 in neuronal differentiation, rat embryos were coelectroporated at embryonic day 17.5 with the EGFP-encoding plasmid together with a vector expressing full-length KCC2 (see Materials and Methods). Immunohistochemical analysis at PND 3, when endogenous expression of KCC2 is low in the cerebral cortex, revealed that the vast majority (>99%) of EGFP-positive pyramidal neurons also strongly express KCC2 (Fig. 3*B*), thereby demonstrating the efficacy of this cotransfection approach.

To determine the impact of the precocious KCC2 expression on dendritic arbor development, layer 2/3 pyramidal neurons expressing KCC2/EGFP-positive as well as adjacent sham controls were iontophoretically injected with LY at PND 10, 15, and 90. Subsequent tracing and analysis of dendritic arbor revealed no difference between control and KCC2/EGFP cells at any of these developmental stages either on apical or basal dendritic tree (Fig. 3*C–D*), providing evidence that premature expression of KCC2 does not affect the maturation of dendritic length and branching.

In contrast, confocal analysis of dendritic spine density on second order shafts of layer 2/3 pyramidal neurons revealed important and lasting differences between control and KCC2/EGFP-expressing neurons. At PND10, overexpression of KCC2 was associated with a 57 ± 16% increase in apical ($P = 0.014$) and a 68 ± 16% increase in basal ($P < 0.0001$) dendritic spine density (Fig. 4*A*). Although increase in spine density between control and KCC2-expressing cells remained in the same order of magnitude at PND 15 on apical (42 ± 8%; $P = 0.0084$) and basal (64 ± 17%; $P = 0.017$) dendritic shafts, it further increased by PND 90 (96 ± 10%; $P = 0.0007$ on apical; and 92 ± 11%; $P = 0.0009$ on basal shafts). These results point to a highly specific spine-targeted action of KCC2 on neuronal structures.

To gain further insights into the consequences of KCC2 overexpression on spinogenesis, and since correlation between spine head volume and synaptic strength has been extensively demonstrated (Arellano et al. 2007; Bourne and Harris 2008), we next assessed how premature expression of KCC2 affects the morphology of dendritic spine heads. As a correlate of the spine head volume, we measured the maximal cross sectional diameter of the protrusion head as determined by analysis of confocal image stacks (see Materials and Methods). This approach revealed that, at any developmental stage studied, increases in dendritic spine density induced by KCC2 expression were not limited to any specific spine population but rather extended to the entire array of spines from small to larger head diameters (Fig. 4).

Increases in Dendritic Spine Density Induced by Premature Expression of KCC2 Are Associated with Increased Spontaneous Excitatory Synaptic Activity

To determine whether KCC2-induced increases in dendritic spine density are associated with an enhancement of the frequency of mEPSCs, we performed whole-cell recordings in the presence of 2 μM TTX and 20 μM bicuculline from KCC2/EGFP-positive and EGFP-negative layer 2/3 pyramidal neurons. Data were obtained from 12 pairs of transfected and non-transfected neurons recorded in the same slice preparations. Consistent with the increased dendritic spine density (Fig. 4*A*), there was a significantly higher frequency of mEPSCs in KCC2/

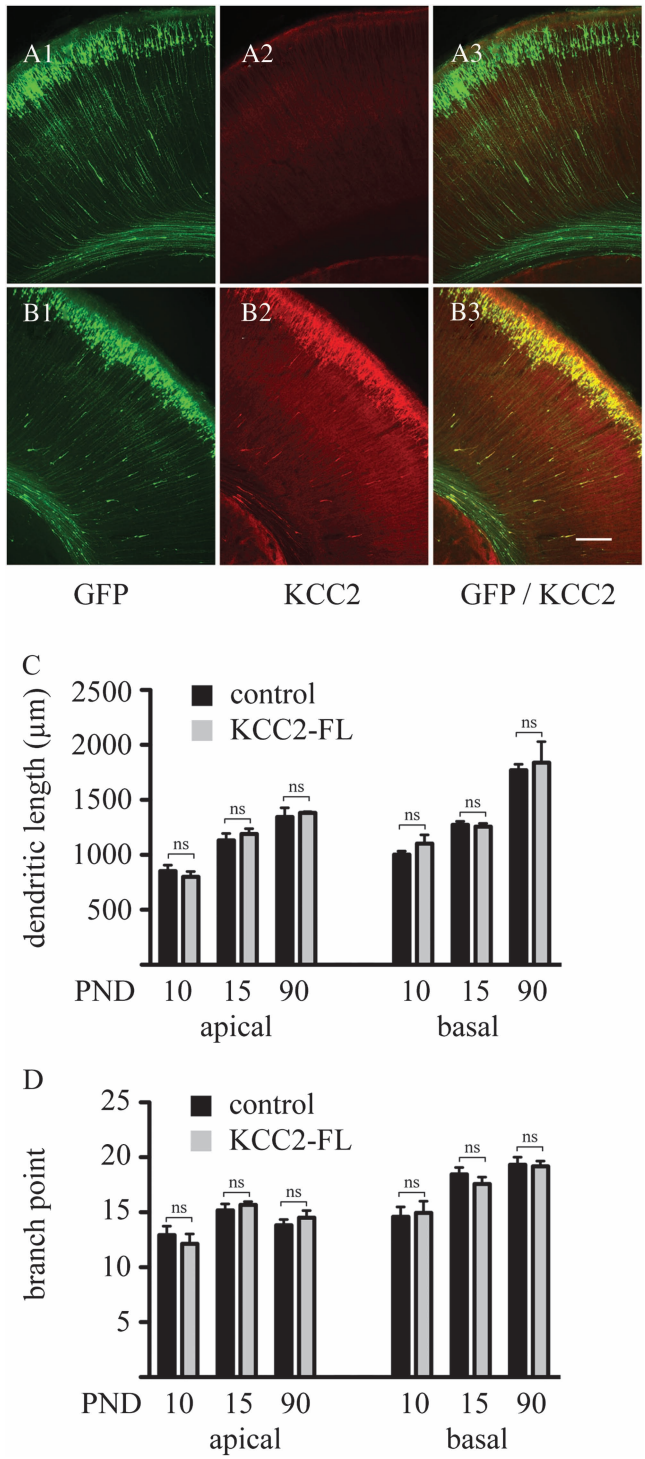

Figure 3. In utero coelectroporation of EGFP and KCC2 does not affect dendritic arbor development of layer 2/3 pyramidal neurons. In contrast to the electroporation of GFP alone (*A*), coelectroporation of EGFP and the KCC2 transporter (*B*) leads to a strong expression of KCC2 in the vast majority of EGFP-positive cells. Quantitative analysis of dendritic length (*C*) and branch points (*D*) shows no effect of KCC2 on the development of gross dendritic structure. Controls represent nonelectroporated LY-injected cells from the same animals, where KCC2 was electroporated. Results are expressed as mean ± standard error of mean, $n = 3$ animals per experimental group. A total of 8–12 injected cells per experimental group were randomly selected for arbor analysis. Within the same developmental age groups, Student's *t*-test was used to examine statistical differences between treatment groups. EGFP, enhanced green fluorescent protein. ns: nonsignificant difference. Scale bar: 100 μm.

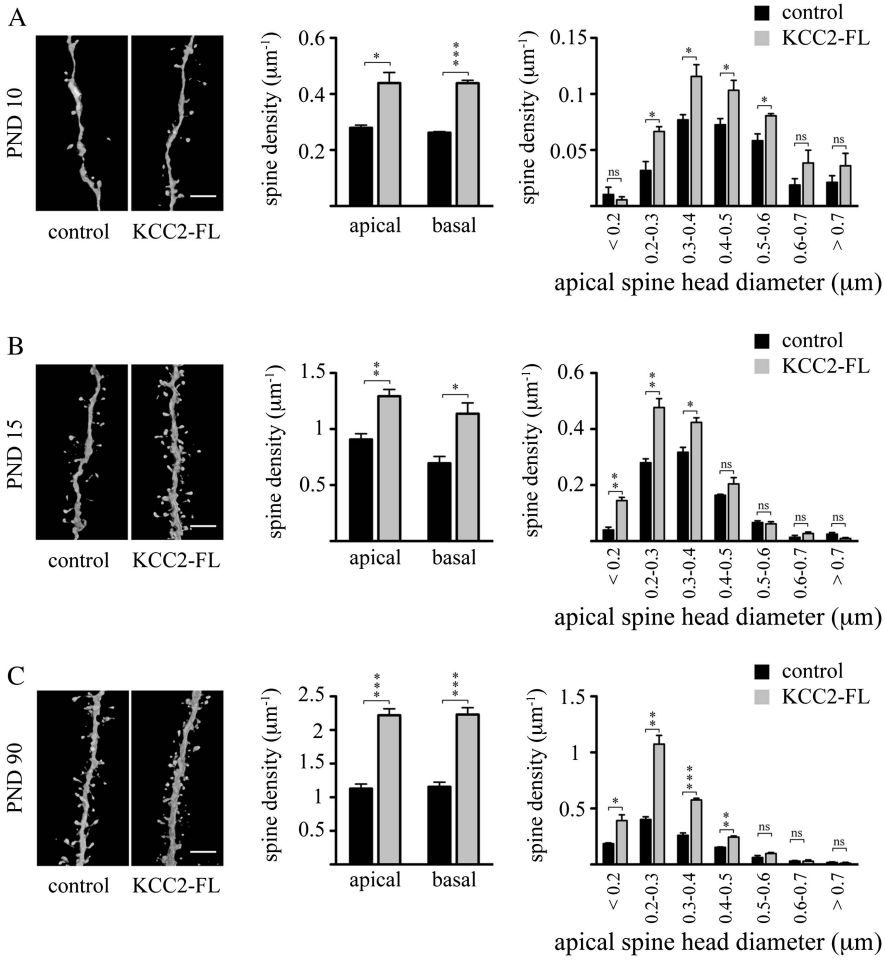

Figure 4. Premature expression of KCC2 increases dendritic spine densities. Representative confocal images (left panels) together with quantitative analyses of apical and basal spine densities (middle panels) as well as spine head diameters (right panels) on PNDs 10 (*A*), 15 (*B*), and 90 (*C*) reveal that KCC2 induces a significant increase in the dendritic spine density at all these developmental stages. Three animals per age group were used to determine spine density for each experimental condition. Controls represent nonelectroporated LY-injected cells from the same animals where KCC2 was electroporated. Results are expressed as mean ± standard error of mean, $n = 3$ animals per group. A total of 5165 spines in controls and of 7543 spines in the KCC2 group was counted to determine spine densities. Within the same developmental age group, Student's *t*-test was used to examine statistical differences between treatment groups. $^{*}P < 0.05$; $^{**}P < 0.01$; $^{***}P < 0.001$ compared with the apical spine density of the control group at the same developmental stage. KCC2-FL, full length KCC2; ns, nonsignificant difference. Scale bar: 6 μm.

EGFP-positive neurons compared with neighboring control neurons (1.96 ± 0.45 and 1.15 ± 0.21 Hz, respectively; $P = 0.0076$; Fig. 5*B*). In contrast, there was no difference in mEPSC amplitude (13.93 ± 0.2 and 13.96 ± 0.27 pA, respectively; $P = 0.88$; Fig. 5*C*).

The Effect of Premature KCC2 Expression on Dendritic Spinogenesis Is Independent of its Chloride Transport Function but Depends on the Actin Binding Capacity of This Protein

KCC2 controls the electrochemical Cl^- gradient and thus the nature of GABAergic responses by actively extruding Cl^- from neurons (Blaesse et al. 2009). To investigate whether the chloride transport function is required for the increased dendritic spinogenesis induced by premature KCC2 expression, we examined the effect of a mutant form of KCC2 lacking the N-terminal domain (KCC2-ΔNTD). This mutant form of KCC2 has been previously shown to be devoid of chloride transport capacity (Li et al. 2007). As shown in Figure 6, in utero electroporation of KCC2-ΔNTD into precursors of layer 2/3 pyramidal neurons significantly increased dendritic spine density determined at PND 10 (apical: +95 ± 19%, $P = 0.013$; basal: +65 ± 15%, $P = 0.014$), at PND 15 (apical: +51 ± 6%, $P = 0.003$; basal: +43 ± 8%, $P = 0.003$) and at PND 90 (apical: +66 ± 6%, $P = 0.001$; basal: +70 ± 12%, $P = 0.002$). Importantly, the distribution pattern of spine head diameters was similar to that observed with the full-length KCC2 construct (Fig. 6*C*,*D*). Together, these results indicate that the effect of premature expression of KCC2 on dendritic spinogenesis is independent of its chloride transporter function.

In vitro evidence suggests that KCC2 promotes dendritic spinogenesis via its interaction with the actin cytoskeleton (Li et al. 2007). To address this issue in vivo, precursors of layer 2/3 pyramidal neurons were electroporated at E17.5 with a KCC2 loss-of-function mutant containing a cysteine-to-alanine substitution at amino acid 568 (KCC2-C568A). KCC2-C568A displays disrupted chloride transport function (Cancedda et al. 2007) and is incapable of interacting with the cytoskeleton-associated structural protein 4.1N, which links KCC2 to the actin cytoskeleton (Li et al. 2007; Horn et al. 2010). As shown in Figure 7, expression of KCC2-C568A in layer 2/3 pyramidal

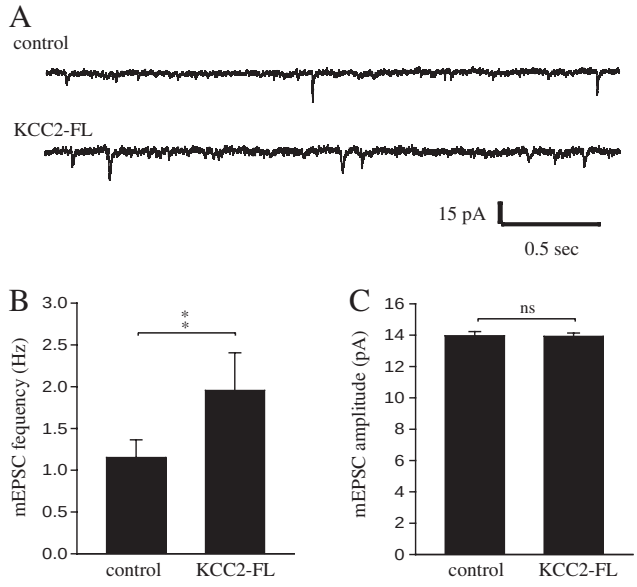

Figure 5. In utero electroporation of KCC2 leads to an increase in the frequency of miniature excitatory currents. (*A*) Traces showing recordings of mEPSCs in non-EGFP-positive (control) and KCC2-FL/EGFP-positive (KCC2-FL) neurons. KCC2-FL neurons ($n = 12$) display a higher frequency (*B*) but not amplitude (*C*) of mEPSCs in comparison to control neurons ($n = 12$). Data are presented as mean ± standard error of mean. Controls represent nonelectroporated cells from the same animals where KCC2 was electroporated. $^{**}P < 0.01$; ns, nonsignificant difference.

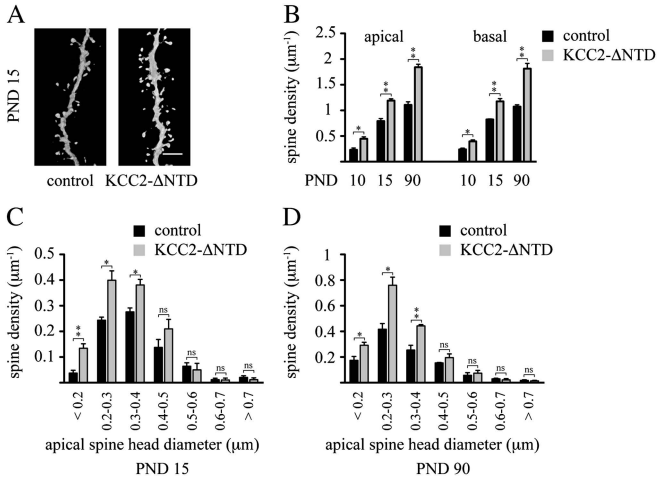

Figure 6. Effect of the non–chloride-extruding deletion construct, KCC2-ΔNTD, on dendritic spinogenesis. (*A*) Representative confocal images (3D volume rendering) showing the impact of the expression of the N-terminal deleted, non–chloride-extruding mutation of the KCC2 transporter on dendritic spinogenesis at PND 15. Quantitative analysis of spine densities (*B*) as well as spine head diameters on PND 15 (*C*) and PND 90 (*D*). Three animals per age group were used to determine spine density for each experimental condition. Controls represent nonelectroporated, LY-injected cells from the same animals, where KCC2-ΔNTD was electroporated. Results are expressed as mean ± standard error of mean, $n = 3$ animals per group. A total of 4928 spines in controls and of 6762 spines in the KCC2-ΔNTD group was counted to determine spine densities. Within the same developmental age group, Student's *t*-test was used to examine statistical differences between treatment groups. $^{*}P < 0.05$; $^{**}P < 0.01$; $^{***}P < 0.001$ compared with the apical spine density of the control group at the same developmental stage. KCC2-ΔNTD, N-terminal deleted form of KCC2; ns, nonsignificant difference. Scale bar: 6 μm.

neurons did not induce any significant increase in dendritic spine density, and the dendritic spine head distribution remained comparable to control neurons at all developmental stages

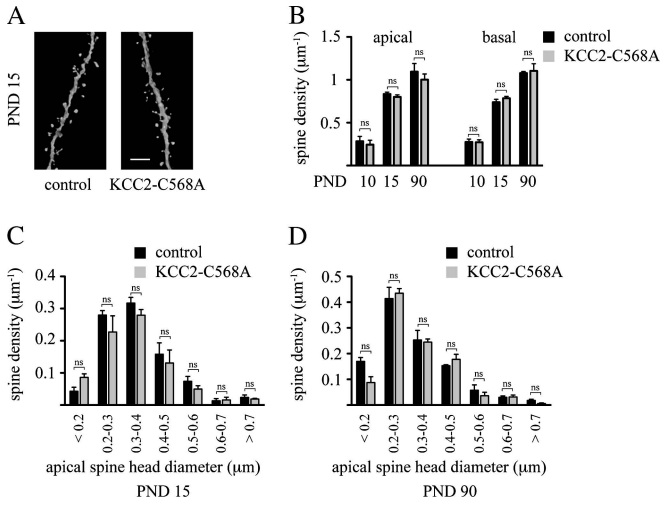

Figure 7. Expression of the KCC2-C568A mutant does not impair dendritic spinogenesis. (*A*) Representative confocal images (3D volume rendering) showing the impact of the KCC2-C568A mutant on dendritic spinogenesis at PND 15. Quantitative analysis of spine densities (*B*) as well as spine head diameters on PND 15 (*C*) and PND 90 (*D*). Three animals per age group were used to determine spine density for each experimental condition. Controls represent nonelectroporated LY-injected cells from the same animals, where KCC2-C568A was electroporated. Results are expressed as mean ± standard error of mean, $n = 3$ animals per group. A total of 3427 spines in controls and of 3502 spines in the KCC2-C568A group was counted to determine spine densities. Within the same developmental age group, Student's *t*-test was used to examine statistical differences between treatment groups. Scale bar: 6 μm. ns: nonsignificant difference.

examined. Data from these studies strongly support a role for an interaction between KCC2 and proteins associated with the dendritic cytoskeleton in the promotion of dendritic spinogenesis.

To gather in vivo experimental evidence substantiating the idea that KCC2 affects spinogenesis by interacting with cytoskeletal proteins via its C-terminal domain, we took advantage of a KCC2 C-terminal domain expression vector (KCC2-CTD) encoding intracellular amino acids 637 through 1116 (Li et al. 2007), with the anticipation that KCC2-CTD will bind to intracellular ancillary cytoskeletal proteins recapitulating the full-length KCC2 effects on spinogenesis. When in utero electroporation was performed at E17.5 with KCC2-CTD, we found that, similar to full-length KCC2, expression of KCC2-CTD increases dendritic spine density on layer 2/3 pyramidal neurons at PND 10, 15, and 90 (Fig. 8). At PND 10, our data revealed 76 ± 9% ($P = 0.0008$) and 96 ± 13% ($P = 0.0011$) increases in spine density on apical and basal dendrites, respectively, in neurons expressing KCC2-CTD compared with control cells. A comparable magnitude of KCC2-CTD–induced increase in dendritic spine density was also observed at later time points (at PND 15: +67 ± 5%, $P = 0.0003$ on apical and +41 ± 2%, $P = 0.0001$ on basal shafts; at PND 90: +82 ± 5%, $P = 0.0008$ on apical and +72 ± 8%, $P = 0.0026$ on basal shafts). In addition, the distribution of dendritic spine head diameters induced by expression of KCC2-CTD was similar to that observed after KCC2 expression. Taken together, our in vivo data are consistent with the notion that the transporter function of KCC2 is not required for increased spinogenesis of cortical pyramidal neurons and indicate that the C-terminal portion of KCC2 interacts with intracellular proteins to increase dendritic spine density.

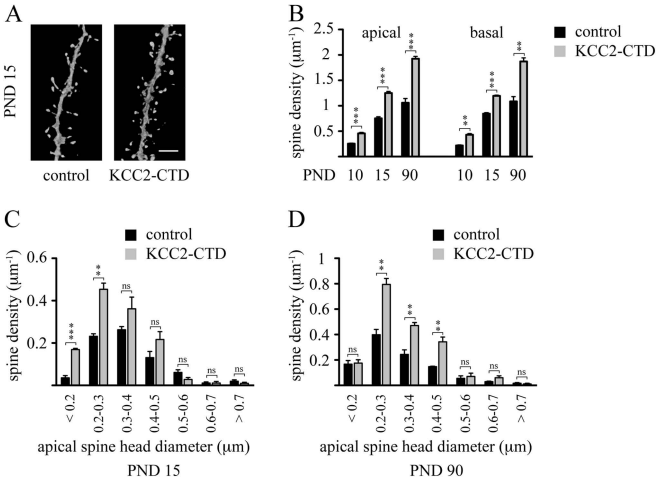

Figure 8. Expression of the C-terminal domain of KCC2 (KCC2-CTD) also increases dendritic spine densities. (*A*) Representative confocal images (3D volume rendering) showing the impact of the expression of the C-terminal form of KCC2 on dendritic spinogenesis at PND 15. Quantitative analysis of spine density (*B*) as well as spine head diameter on PND 15 (*C*) and PND 90 (*D*). Three animals per age group were used to determine spine density for each experimental condition. Controls represent nonelectroporated LY-injected cells from the same animals, where KCC2-CTD was electroporated. Results are expressed as mean ± standard error of mean, $n = 3$ animals per group. A total of 5174 spines in controls and of 7276 spines in the KCC2-CTD group was counted to determine spine densities. Within the same developmental age group, Student's *t*-test was used to determine statistical difference between treatment groups. $^{*}P < 0.05$; $^{**}P < 0.01$; $^{***}P < 0.001$ compared with the apical spine density of the control group at the same developmental stage. KCC2-CTD, C-terminal form of KCC2. Scale bar: 6 μm. ns, nonsignificant difference.

Discussion

In this study, we found that premature expression of KCC2 in layer 2/3 pyramidal neurons in vivo permanently increases the number of spines both on apical and basal dendritic shafts. Whole-cell recordings from cortical pyramidal neurons in acute slices showed that the KCC2-induced increase in spinogenesis was accompanied by an enhancement of the mEPSCs frequency. Moreover, increased spine density was also observed following expression of an ion transport-deficient mutant form of KCC2 (KCC2-ΔNTD). In marked contrast, in utero electroporation of KCC2-C568A, a mutant that does not have the ability to interact with the cytoskeleton, did not affect spine density. Consistent with this observation, precocious expression of the C-terminal domain of KCC2 that mediates interactions with ancillary cytoskeletal proteins, also led to an enhancement of dendritic spine number. Taken together, these results indicate that KCC2 promotes the structural formation of functional excitatory spine synapses during the development of cortical neurons in vivo by a mechanism that is independent of its ion cotransport activity but that requires interactions with cytoskeletal elements.

Our conclusion that the KCC2 effects on spinogenesis depend on an interaction with elements of the spine cytoskeleton but not on the ion transport function of KCC2 is based on data obtained using three functional mutants of KCC2. Premature expression of KCC2-ΔNTD, a deletion mutant form of KCC2 that has been shown previously to lack the chloride transport function but that can interact with the actin cytoskeleton (Li et al. 2007; Horn et al. 2010), increased spine density to values comparable to those found with full-length KCC2 (Fig. 6). Spine density was not affected upon expression of the point mutant KCC2-C568A (Fig. 7), which lacks the transporter function (Cancedda et al. 2007; Reynolds et al. 2008) and the ability to interact with the cytoskeleton (Horn et al. 2010), pointing to the importance of an interaction between KCC2 and the dendritic cytoskeleton to induce spinogenesis. Ectopic expression of the C-terminal domain of KCC2, that mediates the interactions with ancillary cytoskeletal proteins (Li et al. 2007), also led to an enhancement of dendritic spine number (Fig. 8), indicating that the C-terminal domain-mediated scaffolding effects of KCC2 is sufficient to promote spinogenesis. Taken together, these observations indicate that KCC2 stimulates the formation of dendritic spines in vivo by a mechanism that is independent of its ion cotransport activity but that requires interactions with cytoskeletal elements. An important question that remains to be addressed is the molecular mechanism through which KCC2 exerts this structural effect on spines. In this context, it has been shown that the C-terminal domain of KCC2 interacts with the actin cytoskeleton via the cytoskeleton-associated protein 4.1N (Li et al. 2007; Horn et al. 2010). Protein 4.1 family members are linkers known to anchor various ion transporters to the cytoskeletal network of actin and spectrin (Bennett and Baines 2001; Denker and Barber 2002). In line with this observation, plasma membrane insertion and stabilization of GluR1-containing AMPA receptors depend on interactions with the protein 4.1N (Coleman et al. 2003; Lin et al. 2009). Interestingly, it has recently been shown that plasmalemmal KCC2 regulate the postsynaptic AMPA receptor content and lateral diffusion in dendritic spines (Gauvain et al. 2011). It is also important to note that the structural role of KCC2 on dendritic spinogenesis, as observed in the present work, might be restricted to the cerebral cortex, since recent results suggest no effect of genetic manipulation of KCC2 expression during development on dendritic spine densities in the cerebellum (Seja et al. 2012).

In our study, we examined the dendritic architecture of developing layer 2/3 pyramidal neurons of the SSC and found that, while dendritic growth persists over a prolonged period of postnatal life, the complexity of dendritic arbor reaches a stable level by the end of the second postnatal week. These observations are in-line with and complete previous studies performed in rodents where layer 5 pyramidal neurons show similar developmental patterns of dendritic growth and branching in sensorimotor and visual cortices (Juraska 1982; Petit et al. 1988; Uylings et al. 1994). In addition, CA1 pyramidal neurons in the rodent hippocampus show a comparable developmental time course of dendritic growth (Pokorny and Yamamoto 1981), which has been shown to be regulated by neuronal activity (Groc et al. 2002, 2003). Compared with rodents, pyramidal neuron development in primates exhibits marked region specificity in the cerebral cortex. For example, dendritic tree of layer 3 pyramidal neurons in the macaque monkey inferotemporal cortex continues to extend well beyond the peak synaptogenic period, in contrast to the visual cortex (Elston et al. 2010). Importantly, both in rodents and primates, the intense phase of dendritic growth and branching of pyramidal neurons precedes the exponential phase of synaptogenesis (Juraska 1982; Khazipov et al. 2001). Recent observations on dendritic development in the human cerebral cortex indicate layer-specific differences in arbor development (Petanjek et al. 2008). Indeed, while layer 5 pyramidal cells attain their near-adult arborization pattern by the end of the

first postnatal year, layer 3 principal neurons display a second growth spurt period starting at the end of the second year and continuing into the third year of life. Also, large differences in dendritic spine densities have been reported across different cortical regions in the human cerebral cortex that might reflect significant differences in the nature of cortical processing between higher and lower cortical levels (Jacobs et al. 2001).

Our data did not reveal any effect of premature KCC2 expression on gross dendritic structure in layer 2/3 pyramidal neurons (Fig. 2), indicating that the structural influence of KCC2 is limited to spine density. These observations are in contrast with an earlier report (Cancedda et al. 2007), where similar genetic manipulations resulted in impairments of dendrite maturation. This discrepancy could be due to the use of different methods to visualize the dendrites. Here, unbiased analysis of the dendritic morphology of control, EGFP and KCC2/EGFP-expressing neurons was achieved by intracellular LY filling of neurons, whereas, in the other study (Cancedda et al. 2007), visualization of the morphology was based on the EGFP expressed from bicistronic plasmids. In this context, it is important to note that expression levels of markers (e.g., EGFP) downstream of the internal ribosomal entry site (IRES) are known to vary depending on whether a gene is inserted upstream of the IRES (Attal et al. 1999; Houdebine and Attal 1999; Mizuguchi et al. 2000). In contrast, signals from filling dyes are independent from experimental conditions and are considered reliable and accurate for tracing neuronal morphology (Elston et al. 2005).

Data from our study strongly suggest a causal link between KCC2 expression and excitatory synaptogenesis in the cerebral cortex. In line with our observations, the peak period of synaptogenesis in the developing brain of rodents and humans (De Felipe et al. 1997; Huttenlocher and Dabholkar 1997) coincides with a sharp increase in the expression of KCC2 (Rivera et al. 1999; Vanhatalo et al. 2005; Hyde et al. 2011). Moreover, immunohistochemical studies showed a strikingly high level of KCC2 expression in the vicinity of excitatory synapses and in dendritic spines (Gulyas et al. 2001; Baldi et al. 2010). Recent in vitro experiments by Li et al. (2007) have provided evidence suggesting a role for KCC2 in excitatory synaptogenesis. In these studies, neurons from organotypic or dissociated cortical cultures from KCC2 knockout mice showed altered morphology of dendritic spines and exhibited a reduced number of functional excitatory synapses as revealed by reduction of expression levels of excitatory synaptic markers, the number of active presynaptic elements as well as frequency of mEPSCs. Together these observations suggest that KCC2 plays an important role in the formation of excitatory synapses.

Our data indicate that the KCC2-induced increase in spine density was accompanied by an enhancement of functional excitatory synapses. This conclusion is based on our electrophysiological recordings where we found elevated frequency but no change in amplitude of mEPSCs in KCC2-expressing neurons compared with control neurons (Fig. 5). Modification of the mEPSC frequency is generally attributable to a change in the number of synaptic sites, whereas alteration in the corresponding amplitude is due to changes in the property of synapses, such as size and/or receptor content. In keeping with these results, although the dispersion of spine shape changed between the developmental stages examined (Fig. 4), reflecting the normal development of synapses, we found that the distribution of spine head diameters was similar between KCC2-expressing neurons and control neurons at all ages examined (Fig. 4). Together, these observations suggest that ectopic expression of KCC2 influences the number of excitatory synapses without affecting their overall properties from the onset of synaptogenesis.

Data from our study revealed that ectopic expression of KCC2 consistently leads to an increase in the number of dendritic spines as early as PND 10. Importantly, the increased spine density persists and is even more pronounced in adult animals. This latter observation is of utmost importance in light of the well-established concept of activity-dependent stabilization and elimination of initially overproduced synaptic contacts at later developmental stages (Changeux and Danchin 1976). Thus, region-specific pruning of synaptic contacts, starting at the onset of puberty and extending into early adulthood, has been broadly described from rodents to humans (Juraska 1982; Rakic et al. 1994; Petanjek et al. 2011). Interference with physiological patterns of synaptic pruning results in a lower or higher synaptic density, and both these situations have been shown to be associated with psychiatric disorders. In fact, synaptic overproduction and incomplete pruning is associated with autism spectrum disorders, while exaggerated pruning during late childhood and adolescence may lead to emergence of symptoms characterizing schizophrenia (for review, see van Spronsen and Hoogenraad 2010; Penzes et al. 2011).

Dendritic spine dynamics depend on the stage of development of the animal. For instance, during early postnatal development, dendritic spines are highly motile and undergo intense turnover (Lendvai et al. 2000). In adults, while spines retain some lability for learning-based plasticity (Yang et al. 2009), they nevertheless display remarkable stability (Bhatt et al. 2009). Aging is accompanied by a progressive synaptic loss in the prefrontal cortex resulting in impaired plasticity at existing synapses (Peters et al. 2008). Interestingly, recent work suggests that stress-induced morphological plasticity observed in the juvenile rodent neocortex is absent in middle-aged and aged animals (Bloss et al. 2010). In this context, the question of how the enhancement of dendritic spine number induced by premature KCC2 expression affects synaptic plasticity and information processing in mature cortical networks remains an intriguing issue.

In conclusion, our study points to an ion transport-independent structural role for KCC2 during excitatory synaptogenesis in cortical pyramidal neurons in vivo. This mechanism may play an important role during activity-dependent assembly of developing cortical circuits and may have functional consequences for adult brain plasticity.

Funding

This study was funded by Swiss National Science Foundation Grants 31003A-124783 (to J-L.M.) and 31003A-130625 (to L.V.) and by the Academy of Finland (to K.K.).

Notes

Conflict of Interest: None declared.

References

Arellano JI, Benavides-Piccione R, Defelipe J, Yuste R. 2007. Ultrastructure of dendritic spines: correlation between synaptic and spine morphologies. Front Neurosci. 1:131–143.

Attal J, Theron MC, Houdebine LM. 1999. The optimal use of IRES (internal ribosome entry site) in expression vectors. Genet Anal. 15:161–165.
Baldi R, Varga C, Tamas G. 2010. Differential distribution of KCC2 along the axo-somato-dendritic axis of hippocampal principal cells. Eur J Neurosci. 32:1319–1325.
Bartho P, Payne JA, Freund TF, Acsady L. 2004. Differential distribution of the KCl cotransporter KCC2 in thalamic relay and reticular nuclei. Eur J Neurosci. 20:965–975.
Bennett V, Baines AJ. 2001. Spectrin and ankyrin-based pathways: metazoan inventions for integrating cells into tissues. Physiol Rev. 81:1353–1392.
Bhatt DH, Zhang S, Gan WB. 2009. Dendritic spine dynamics. Annu Rev Physiol. 71:261–282.
Blaesse P, Airaksinen MS, Rivera C, Kaila K. 2009. Cation-chloride cotransporters and neuronal function. Neuron. 61:820–838.
Bloss EB, Janssen WG, McEwen BS, Morrison JH. 2010. Interactive effects of stress and aging on structural plasticity in the prefrontal cortex. J Neurosci. 30:6726–6731.
Bourne JN, Harris KM. 2008. Balancing structure and function at hippocampal dendritic spines. Annu Rev Neurosci. 31:47–67.
Briner A, De Roo M, Dayer A, Muller D, Habre W, Vutskits L. 2010. Volatile anesthetics rapidly increase dendritic spine density in the rat medial prefrontal cortex during synaptogenesis. Anesthesiology. 112:546–556.
Cancedda L, Fiumelli H, Chen K, Poo MM. 2007. Excitatory GABA action is essential for morphological maturation of cortical neurons in vivo. J Neurosci. 27:5224–5235.
Changeux JP, Danchin A. 1976. Selective stabilisation of developing synapses as a mechanism for the specification of neuronal networks. Nature. 264:705–712.
Coleman SK, Cai C, Mottershead DG, Haapalahti JP, Keinanen K. 2003. Surface expression of GluR-D AMPA receptor is dependent on an interaction between its C-terminal domain and a 4.1 protein. J Neurosci. 23:798–806.
De Felipe J, Marco P, Fairen A, Jones EG. 1997. Inhibitory synaptogenesis in mouse somatosensory cortex. Cereb Cortex. 7:619–634.
De Roo M, Klauser P, Briner A, Nikonenko I, Mendez P, Dayer A, Kiss JZ, Muller D, Vutskits L. 2009. Anesthetics rapidly promote synaptogenesis during a critical period of brain development. PLoS One. 4:e7043.
Denker SP, Barber DL. 2002. Ion transport proteins anchor and regulate the cytoskeleton. Curr Opin Cell Biol. 14:214–220.
Elston GN, Benavides-Piccione R, Defelipe J. 2005. A study of pyramidal cell structure in the cingulate cortex of the macaque monkey with comparative notes on inferotemporal and primary visual cortex. Cereb Cortex. 15:64–73.
Elston GN, Oga T, Okamoto T, Fujita I. 2010. Spinogenesis and pruning from early visual onset to adulthood: an intracellular injection study of layer III pyramidal cells in the ventral visual cortical pathway of the macaque monkey. Cereb Cortex. 20:1398–1408.
Fiumelli H, Cancedda L, Poo MM. 2005. Modulation of GABAergic transmission by activity via postsynaptic Ca2+-dependent regulation of KCC2 function. Neuron. 48:773–786.
Gauvain G, Chamma I, Chevy Q, Cabezas C, Irinopoulou T, Bodrug N, Carnaud M, Levi S, Poncer JC. 2011. The neuronal K-Cl cotransporter KCC2 influences postsynaptic AMPA receptor content and lateral diffusion in dendritic spines. Proc Natl Acad Sci U S A. 108:15474–15479.
Groc L, Petanjek Z, Gustafsson B, Ben-Ari Y, Hanse E, Khazipov R. 2002. In vivo blockade of neural activity alters dendritic development of neonatal CA1 pyramidal cells. Eur J Neurosci. 16:1931–1938.
Groc L, Petanjek Z, Gustafsson B, Ben-Ari Y, Khazipov R, Hanse E. 2003. Compensatory dendritic growth of CA1 pyramidal cells following growth impairment in the neonatal period. Eur J Neurosci. 18:1332–1336.
Gulyas AI, Sik A, Payne JA, Kaila K, Freund TF. 2001. The KCl cotransporter, KCC2, is highly expressed in the vicinity of excitatory synapses in the rat hippocampus. Eur J Neurosci. 13:2205–2217.
Harris KM, Stevens JK. 1989. Dendritic spines of CA 1 pyramidal cells in the rat hippocampus: serial electron microscopy with reference to their biophysical characteristics. J Neurosci. 9:2982–2997.
Hensch TK. 2004. Critical period regulation. Annu Rev Neurosci. 27:549–579.
Horn Z, Ringstedt T, Blaesse P, Kaila K, Herlenius E. 2010. Premature expression of KCC2 in embryonic mice perturbs neural development by an ion transport-independent mechanism. Eur J Neurosci. 31:2142–2155.
Houdebine LM, Attal J. 1999. Internal ribosome entry sites (IRESs): reality and use. Transgenic Res. 8:157–177.
Huttenlocher PR, Dabholkar AS. 1997. Regional differences in synaptogenesis in human cerebral cortex. J Comp Neurol. 387:167–178.
Hyde TM, Lipska BK, Ali T, Mathew SV, Law AJ, Metitiri OE, Straub RE, Ye T, Colantuoni C, Herman MM, et al. 2011. Expression of GABA signaling molecules KCC2, NKCC1, and GAD1 in cortical development and schizophrenia. J Neurosci. 31:11088–11095.
Jacobs B, Schall M, Prather M, Kapler E, Driscoll L, Baca S, Jacobs J, Ford K, Wainwright M, Treml M. 2001. Regional dendritic and spine variation in human cerebral cortex: a quantitative golgi study. Cereb Cortex. 11:558–571.
Juraska JM. 1982. The development of pyramidal neurons after eye opening in the visual cortex of hooded rats: a quantitative study. J Comp Neurol. 212:208–213.
Khazipov R, Esclapez M, Caillard O, Bernard C, Khalilov I, Tyzio R, Hirsch J, Dzhala V, Berger B, Ben-Ari Y. 2001. Early development of neuronal activity in the primate hippocampus in utero. J Neurosci. 21:9770–9781.
Kwon HB, Sabatini BL. 2011. Glutamate induces de novo growth of functional spines in developing cortex. Nature. 474:100–104.
Lendvai B, Stern EA, Chen B, Svoboda K. 2000. Experience-dependent plasticity of dendritic spines in the developing rat barrel cortex in vivo. Nature. 404:876–881.
Li H, Khirug S, Cai C, Ludwig A, Blaesse P, Kolikova J, Afzalov R, Coleman SK, Lauri S, Airaksinen MS, et al. 2007. KCC2 interacts with the dendritic cytoskeleton to promote spine development. Neuron. 56:1019–1033.
Lin DT, Makino Y, Sharma K, Hayashi T, Neve R, Takamiya K, Huganir RL. 2009. Regulation of AMPA receptor extrasynaptic insertion by 4.1N, phosphorylation and palmitoylation. Nat Neurosci. 12:879–887.
LoTurco J, Manent JB, Sidiqi F. 2009. New and improved tools for in utero electroporation studies of developing cerebral cortex. Cereb Cortex. 19(Suppl 1):i120–i125.
Mizuguchi H, Xu Z, Ishii-Watabe A, Uchida E, Hayakawa T. 2000. IRES-dependent second gene expression is significantly lower than cap-dependent first gene expression in a bicistronic vector. Mol Ther. 1:376–382.
Niwa H, Yamamura K, Miyazaki J. 1991. Efficient selection for high-expression transfectants with a novel eukaryotic vector. Gene. 108:193–199.
Nusser Z, Lujan R, Laube G, Roberts JD, Molnar E, Somogyi P. 1998. Cell type and pathway dependence of synaptic AMPA receptor number and variability in the hippocampus. Neuron. 21:545–559.
Penzes P, Cahill ME, Jones KA, VanLeeuwen JE, Woolfrey KM. 2011. Dendritic spine pathology in neuropsychiatric disorders. Nat Neurosci. 14:285–293.
Petanjek Z, Judas M, Kostovic I, Uylings HB. 2008. Lifespan alterations of basal dendritic trees of pyramidal neurons in the human prefrontal cortex: a layer-specific pattern. Cereb Cortex. 18:915–929.
Petanjek Z, Judas M, Simic G, Rasin MR, Uylings HB, Rakic P, Kostovic I. 2011. Extraordinary neoteny of synaptic spines in the human prefrontal cortex. Proc Natl Acad Sci U S A. 108:13281–13286.
Peters A, Sethares C, Luebke JI. 2008. Synapses are lost during aging in the primate prefrontal cortex. Neuroscience. 152:970–981.
Petit TL, LeBoutillier JC, Gregorio A, Libstug H. 1988. The pattern of dendritic development in the cerebral cortex of the rat. Brain Res. 469:209–219.
Pokorny J, Yamamoto T. 1981. Postnatal ontogenesis of hippocampal CA1 area in rats. I. Development of dendritic arborisation in pyramidal neurons. Brain Res Bull. 7:113–120.

Rakic P, Bourgeois JP, Goldman-Rakic PS. 1994. Synaptic development of the cerebral cortex: implications for learning, memory, and mental illness. Prog Brain Res. 102:227–243.

Reynolds A, Brustein E, Liao M, Mercado A, Babilonia E, Mount DB, Drapeau P. 2008. Neurogenic role of the depolarizing chloride gradient revealed by global overexpression of KCC2 from the onset of development. J Neurosci. 28:1588–1597.

Rivera C, Voipio J, Payne JA, Ruusuvuori E, Lahtinen H, Lamsa K, Pirvola U, Saarma M, Kaila K. 1999. The K+/Cl- co-transporter KCC2 renders GABA hyperpolarizing during neuronal maturation. Nature. 397:251–255.

Saito T, Nakatsuji N. 2001. Efficient gene transfer into the embryonic mouse brain using in vivo electroporation. Dev Biol. 240:237–246.

Schikorski T, Stevens CF. 1999. Quantitative fine-structural analysis of olfactory cortical synapses. Proc Natl Acad Sci U S A. 96:4107–4112.

Schikorski T, Stevens CF. 2001. Morphological correlates of functionally defined synaptic vesicle populations. Nat Neurosci. 4:391–395.

Seja P, Schonewille M, Spitzmaul G, Badura A, Klein I, Rudhard Y, Wisden W, Hubner CA, De Zeeuw CI, Jentsch TJ. Forthcoming 2012. Raising cytosolic Cl^- in cerebellar granule cells affects their excitability and vestibulo-ocular learning. EMBO J. 2012 Jan 17. doi: 10.1038/emboj.2011.488. [Epub ahead of print].

Uylings HB, van Pelt J, Parnavelas JG, Ruiz-Marcos A. 1994. Geometrical and topological characteristics in the dendritic development of cortical pyramidal and non-pyramidal neurons. Prog Brain Res. 102:109–123.

Yang G, Pan F, Gan WB. 2009. Stably maintained dendritic spines are associated with lifelong memories. Nature. 462(7275): 920–924.

van Spronsen M, Hoogenraad CC. 2010. Synapse pathology in psychiatric and neurologic disease. Curr Neurol Neurosci Rep. 10:207–214.

Vanhatalo S, Palva JM, Andersson S, Rivera C, Voipio J, Kaila K. 2005. Slow endogenous activity transients and developmental expression of K+-Cl- cotransporter 2 in the immature human cortex. Eur J Neurosci. 22:2799–2804.